A comparison of landslide inventories produced by manual and automated methods on timberlands in the Pacific Northwest

Patrick Faha

A report prepared in partial fulfillment of
the requirements for the degree of

Master of Science
Earth and Space Sciences: Applied Geosciences

University of Washington

June, 2017

Project mentor:
Orv Mowry

Internship coordinator:
Kathy Troost

Reading committee:
Juliet Crider
Steven Walters

MESSAGe Technical Report Number: [053]

Acknowledgements

I owe this degree and much gratitude to everyone who has been involved with my experience at the University of Washington. Dr. Kathy Troost for acting as internship coordinator and introducing me to the partner organization. The partner organization for granting me access to their facilities and data, and inspiring the development of this project. Dr. Steven Walters for his guidance and suggestions on geospatial techniques. Dr. Juliet Crider for her unending commitment to MESSAGe and its students and guiding me through some of the most difficult parts of this project. Finally, I would like to thank my parents, who challenged me to pursue a graduate degree and without whom this would not have been possible.

Table of Contents page

Executive Summary

Landslides can threaten the potential value of total production on timberlands either by destroying a present crop or by inhibiting future growth. To mitigate or prevent such loss of value due to landslides, it is essential to identify past and existing mass movement events. This is accomplished through the creation and maintenance of a landslide inventory map. Through this project, I partnered with a timber company to create a landslide inventory of their existing properties in Washington and Oregon. I used two methods to create the inventory and compared the results. This inventory will facilitate and guide the decision making process when considering properties for harvest, sale, or development.

Traditional methods for identifying landslides area all conducted manually. These range from field investigations to interpretation of aerial imagery and elevation derived maps. Traditional methods suffer from a lack of a standardized method and because they are inherently subjective. Newer landslide identification methods can be performed automatically. These are typically based on roughness calculations or classifications of spectral imagery. Automated methods continue to be developed and still need refinement before being considered as a replacement for manual mapping.

Using high resolution LiDAR imagery, I created a manually identified landslide inventory through visual interpretation of a bare earth surface. I used the same LiDAR imagery and a roughness calculation based on a continuous wavelet transform method to create an automatically identified landslide inventory. The results of these two methods were compared based on total areal coverage, spatial agreement, and overall geographic patterns.

I identified and delineated a total of 470 individual landslides through manual review of all properties. Landslide terrain covered approximately 2.4 percent of the total area evaluated. The automated review did not identify individual landslides, but grouped any adjacent slides together, preventing any evaluation of individual events. In the results of the automated review, slide terrain accounted for 11.5 percent of the total area evaluated. The degree of matching between the two methods equaled 11, 17, 20, and 27 percent in the four subsets of the study area. Most of the mismatch is accounted for areas that were identified by the automated method but not the manual method.

Landslide inventories are inherently incomplete due to the dynamic nature of surface morphology and the potential for unidentified slides. The two methods used in this evaluation present two unique interpretations of the landslides on the partner organization's properties. Further review, both manual and automated, may result in a higher degree of agreement between the methods. Currently, the manual inventory is a reliable identifier of existing slides. The automated inventory worked poorly for identifying individual slides but could be used to guide further investigations into areas that have a higher potential for slides.

Introduction

Removal of vegetation has been shown to have a positive correlation to increases in mass movement events (Furbish & Rice, 1983). As an industry that actively removes vegetation from steep slopes, it is important for tree farms and logging companies to understand the potential for landslides on their properties. The rugged terrain and regular precipitation of the Pacific Northwest make this especially true. Landslide inventory maps are a preliminary assessment tool in any landslide investigation and can be used to record existing slides as well as be incorporated into landslide susceptibility, hazard, and risk assessments of future slides (Guzzetti et al., 2012). Therefore, landslide inventory maps should be an essential consideration when timber companies evaluate properties for sale or development.

Landslide mapping techniques can be characterized as field- or office-based techniques. Office methods can be further characterized as manual and automated. Manual review methods lend the confidence and review of an experienced individual. However, they can also suffer from inexperienced observers, low resolution data, and time constraints. Automated methods are more recent and require further refinement. These can provide a cursory look at terrain that may have failed. Automated methods are also newer and continue to be developed and refined.

This study was conducted in collaboration with a Pacific Northwest timber company. This partner organization requires an up-to-date, comprehensive, deep-seated-landslide inventory map of their existing properties in Washington and Oregon. This inventory will inform and guide decisions regarding landslide hazards as they maintain and review properties for development and harvest. This study undertakes the creation of a manual landslide inventory and an automatic inventory based on ground-surface roughness. The results demonstrate spatial differences in the designation of landslide terrain between the two inventories, revealing variability in effectiveness and accuracy of the manual and automated methods used to detect deep-seated landslide occurrences.

All figures in this report are geographically cropped to a spatially limited area to exclude any distinguishing features. This is due to privacy concerns from the partner organization to prevent recognition of land within their ownership, and because some of the LiDAR imagery used was proprietarily collected.

Field identification of landslides

Geomorphological field mapping is the most rudimentary method of documenting landslides. Mapping is accomplished using conventional field techniques by observing and recording morphological characteristics of past landslides (Guzzetti et al., 2012). Features indicative of a landslide include head and flank scarps, landslide body and toe, and hummocks. (Cruden & Varnes, 1978). In the presence of these primary features, observation of secondary features such as tension cracks and sag ponds can reinforce the designation of a landslide terrain (Cruden & Varnes, 1978; Guzzetti et al., 2012). In addition to morphological mapping, subsidiary observations can be made to confirm the presence of a landslide. Such observations can include the location and growth density of moisture-loving vegetation, standing water, and nearby terrain

features that may contribute to mass wasting such as a concave headland (Cruden and Varnes, 1996).

Field techniques can provide numerous specific supplementary data to indicate landslides. Field mapping methods are particularly effective when investigating single landslides, causes of landslides, and validating inventory maps created using office techniques (Guzzetti et al., 2012). While effective for mapping few landslides over a small area, larger areas present greater challenges to field mapping. Accessibility, time, and cost commitments can all be prohibitive to field mapping (Guzzetti et al., 2012). Because of these challenges, weathering, and vegetation precise boundaries are not always definable (Galli et al., 2007). Field investigations can also lack the widespread and quick coverage an office review (Eeckhaut et al., 2004).

Office review for landslide mapping

Generation of landslide inventory maps using an in-office review has traditionally been performed with the use of aerial photography. Aerial photographs are a reliable resource for the identification of landslides because trained geomorphologists have experience using the medium and can readily recognize the most prominent morphological features of landslides (Guzzetti et al., 2012). Interpretation of physical photographs can be performed cheaply with a stereoscope and a wealth of data collected for many purposes exists through local, state, and federal government archives of aerial photography.

Digital landslide identification can be performed using elevation datasets and their derivative products such as slope and contours. High resolution LiDAR datasets provides effective data to observe changes in surface morphology because of the ability to view the ground surface without vegetation, which can obscure as much as 85% of total failures (Brardinoni et al., 2002). When viewed as a hillshade, these elevation datasets allow users to observe any spatial or temporal changes in topography or morphology at scales greater than the resolution of traditional imagery. The often meter-scale resolution of bare earth LiDAR can provide landslide inventories of a much higher accuracy than traditional aerial photograph interpretation.

The basis of manual landslide mapping via visual interpretation is recognition of characteristic features within and around landslides. These can be recorded in the setting, topography, texture, shape, size, and patterns within the study site. Setting and topography can be controls on external causes and triggers that may result in landslides; such as differences between an arid, unvegetated environment and a humid heavily vegetated area. Texture, shape, size, and patterns can all be used to describe the morphology resultant from a landslide. Identification of features such as the head and flank scarps, transverse cracks, hummocks and swales, and zones of depletion and accumulation are all evidence to support the presence of a landslide.

Advantages of using aerial photograph and surface morphology interpretation are that they allows users to observe large areas which may be affected by landslides, entire landslides can be captured in single images, and they can be used in unison with supporting data such as topographic maps and field observations. This approach greatly reduces the time demanded to create a landslide inventory when compared with field methods. Aerial photographs can also yield a view of features that may have been impossible to observe in the field due to vegetative

or topographic obstructions or other safety concerns. This complete view, in contrast to field methods, provides the user with the ability to differentiate a landslide feature from a feature of similar structure by observing other features on nearby terrain. The overhead view also allows users to delineate the complete affected area without having to identify boundaries by walking the perimeter of the landslide.

The primary disadvantage of aerial photograph or terrain interpretation is that there is no universally accepted standard by which to map. All designation of landslides is dependent on the user's own experience and subjective ability to recognize and delineate landslide morphology. Data availability can also vary greatly from location to location, resulting in inventories created at different scales, resolution, and completeness. The process can be time consuming and requires complete manual evaluation of the study area. This creates the potential for overlooking unrecognized or highly weathered landslides, misidentifying landslides as non-landslides, and misidentifying non-landslides as landslides.

Automated landslide mapping techniques

Several methods have been developed for automated landslide mapping. Because landslides leave a characteristic roughness signature, surface roughness calculations can be used to approximately define failed terrain (Van Den Eeckhaut, 2005; Booth et al., 2009). Surface roughness can be characterized by simple statistical measures of physical characteristics and by more complex frequency signal processing (Berti et al., 2013). Root means squared measures of height, slope, and aspect, which measure deviations from the normal, are a common method of automatically identifying landslide terrain (Shepard et al., 2001). Booth, et al. (2009) use a discrete Fourier and continuous wavelet transform to identify characteristic spatial frequencies of deep-seated landslides. These are signal processing methods that allow for the simplification of finite frequency signaling that can be convolved to identify landslide terrain.

A different approach to automatic detection uses spectral signatures from satellite imagery. Both optical imagery and synthetic aperture radar (SAR) can be used for automatic landslide identification (Guzzetti et al., 2012). Optical methods rely on the land cover classification and can be conducted through a pixel based or object oriented approach (Mondini et al., 2011; Stumpf & Kerle, 2011). Imagery preprocessing can introduce uncertainty into imagery based methods as the same processes must be performed on all images being analyzed to maintain uniform spectral signatures (Mondini et al., 2011). SAR uses centimeter to millimeter scale accuracy to measure surface deformations in time series analyses (Farina et al., 2006).

Because the study area of this report is forested and a single cumulative inventory is being produced, roughness calculations generated from bare-earth LiDAR imagery is better suited than spectral analysis.

Regional Geologic and Environmental Setting

The study area includes the partner organization properties in western Washington and north western Oregon. These properties range in size from tens of square meters to several square kilometers in area. Though scattered across a large area and with discontiguous borders, the properties can be grouped into "clusters". Three clusters lie within Washington in the approximate areas of Shelton, Brooklyn, and Morton. One cluster lies within Oregon in Clackamas County.

To determine the underlying geology of each cluster in the study, I used the Washington Division of Geology and Earth Resources 1:100,000 series of geologic quadrangle maps (Logan, 2003; Logan, 1987; Phillips, 1987; Schasse, 1987; Walsh, 1987). These maps provide complete and uniform coverage of the study regions. Further investigations into individual landslides should use larger scale maps to differentiate unique geology of different properties within the study area. The geologic descriptions provided below are derived from these maps and the accompanying literature.

Shelton

Properties in the Shelton area are mainly in the south central portion of the quadrangle. The most widespread basement rocks are Eocene marine volcanics of the Crescent Formation. Overlying these are the uplifted marine Oligocene-Eocene tuffaceous siltstone and fine-grained sandstone of the Lincoln Creek Formation which belongs to the Hoh Assemblage. This formation is commonly hackly jointed and has indistinct to massive bedding. The youngest bedrock unit in the area is the Montesano Formation composed of coarse- to fine-grained lithofeldspathic to feldspatholithic sandstone with common conglomerate, siltstone, and mudstone.

The area of focus within the quadrangle has deposits from two recent continental glaciations; an older Wisconsonian glaciation, and the Vashon Stade of the Fraser glaciation (also Wisconsonian). The older of these events has a further southern maximum extent which trends east-west across the properties. Deposits from this maximum extent are laterally discontinuous undifferentiated drift and are located primarily along the bounds of major river valleys and drainage basins. The maximum extent of the Vashon Stade glaciation is north of the older glacial extent and similarly trends east-west. Deposits north of the maximum extent of this younger glaciation overlie the aforementioned bedrock units as a largely continuous till. South of the maximum extent, outwash and other drift deposits from the Vashon Stade are exposed in the lows of drainage basins and fluvial valleys.

Brooklyn

Properties in the Brooklyn area are the most spatially dispersed of all the clusters and fall within the Chehalis, Centralia, Astoria, and Mt. St. Helens geologic quadrangles.

The oldest rocks underlying properties in the area are the mixed nearshore marine to non-marine siltstones and sandstones of the Eocene Cowlitz Formation. Overlying these are the tuffaceous marine siltstones and sandstones of the McIntosh Formation; the nearshore marine to non-marine interbedded shale, siltstone, and sandstone of the Skookumchuck Formation; and the tuffaceous

siltstones and sandstones of the Oligocene-Eocene Lincoln Creek Formation. These three formations belong to the uplifted marine sedimentary rocks of the Hoh Assemblage. The Cowlitz Formation is exposed near the intersection of the four quadrangles and appears in all quadrangles but the Centralia. The McIntosh Formation appears in the Chehalis and Astoria quadrangles, the Skookumchuck Formation appears on the border of the Chehalis and Centralia quadrangles, and the Lincoln Creek Formation appears in the Chehalis and Astoria quadrangles.

Miocene rocks in the area lack the spatial coverage of the Eocene and Oligocene-Eocene aged rocks. Outcrops of the marine coarse to fine-grained, silty, friable, sandstones of the Montesano and fine-grained, silty, friable Astoria Formations are found in the central portion of the Chehalis quadrangle. The Grande Ronde Basalt of the Columbia River Basalt Group, which is composed of continental basalt and andesite flows originating from southeastern Washington and nearby Idaho and Oregon, is exposed as isolated outcrops along the Chehalis River and nearby drainages. A limited number of lows are recorded in these units; the upper flows exhibit well developed columnar structure and the lower flows exhibit will develop entablature structure. These flows extend between the Chehalis and Astoria quadrangles. Continental volcanic lithic bearing sandstones, siltstones, and conglomerates of the Wilkes Formation are found in central Chehalis quadrangle and the St Helens quadrangle.

Surficial geology in the area consists of glacial deposits from alpine and continental sources. Pre-Fraser alpine outwash deposits are differentiated into the Logan Hill, Wingate Hill, and Hayden Creek Formations. Of these, the Logan Hill is the most extensive in the study area and is found in the Centralia and Astoria quadrangles; the Wingate Hill is found in the St Helens quadrangle; and the Hayden Creek is found in the Centralia and St Helens quadrangles. The Fraser Glaciation produced deposits as well in the Evans Creek Formation, which is alpine glacial outwash, and Vashon outwash from continental glaciation. The alpine Evans Creek is only found in the St Helens quadrangle and the continental outwash is only found in the Centralia quadrangle. Quaternary alluvium is found locally in river channels. This series of DNR reports also identifies a number of landslide deposits; these have a high occurrence in areas with Skookumchuck Formation bedrock.

Morton

Properties in the Morton area lie in the Centralia and Mt St Helens quadrangles. The oldest rocks in the area are the Eocene continental sandstones, siltstones, shales, and claystones of the Puget Group. These are interbedded with concurrent basaltic andesite and andesite flows, flow breccia, and sills of the Northcraft Formation. Several stages of later volcanics are found throughout the area, beginning with the Oligocene-Eocene Goble Volcanics which are distinguished as (1) light colored volcaniclastic sandstone, siltstone, conglomerate, lapilli and ash tuff, and breccia and (2) thin basaltic andesite flows and flow breccia with blocky to platy joint sets and wavy contacts and sandstone or siltstone between flows. Less distinct volcanics of similar age consist of porphyritic vesicular basaltic andesite flows with associated volcaniclastic sedimentary rocks. These volcanics are locally interbedded with the late stages of the Puget Group and the Northcraft Formation. Volcanism continued into the Oligocene with the Ohanapecosh Formation; a well indurated unit defined by undifferentiated volcaniclastics and limited lava

flows. Volcanics of the Miocene-Oligocene produced flows and volcaniclastics of basalt, basaltic andesite, andesite, and dacite.

Some of the extrusive flows of the Oligocene-Miocene may be associated with simultaneous intrusive events. These began as andesite and diorite dikes, sills, and plugs. The intrusive andesite exhibits blocky to platy jointing with local alteration to chlorite and zeolite. The early phase of intrusion of the Spirit Lake Pluton emplaced complex dikes and irregular intrusions of granodiorite. Intrusive rocks in the study area are expressed in limited spatially dispersed exposures; andesite and diorite in Centralia and the Spirit Lake granodiorite in Mt St Helens.

Surficial deposits include pre-Fraser age alpine till and outwash of the Hayden Creek Formation and Fraser age alpine till and glacial drift of the Evans Creek Formation.

Oregon

Properties in Oregon are primarily located in west central and southern Clackamas County. Geology of this area is defined by continental sedimentary rocks and extrusive volcanics. The oldest unit in the area are limited exposures of the Oligocene terrestrial sedimentary Scotts Mills Formation, part of the Yaquina-Pittsburg Bluff Group. Volcanics and volcaniclastics of the Little Butte Volcanics are expressed toward the western extent of the study area. Locally interbedded with these and expressed in valley lows are exposures of the Columbia River Basalt Group. The central study area is blanketed by the dominantly andesitic Rhododendron Formation of the Late Western Cascade Volcanics. The northern extent of the study area sees fluvial terrace deposits of mudstone, sandstone, and conglomerate of the Troutdale Formation of the Willamette Group. These are overlain in elevated areas by basalt and basaltic andesite of the Boring Volcanic Field originating from the Portland Basin Volcanoes.

Regional Tectonics

The Pacific Northwest is a tectonically active region with much of this activity attributed to the subduction of the Juan de Fuca Plate under the North American Plate. A number of tectonic and structural features trend generally SE-NW through or near the Washington study areas. The Shelton properties are relatively free of large scale faults with few short faults to the west and south. The Brooklyn properties are nestled within the highest concentration of faults in the study area. Though most properties are absent of large faults, many normal faults and some with indeterminate motion exist nearby the properties and some properties are intersected by these faults. Faults in the Morton area trend in a more E-W direction than in the other areas. There are not many faults in this area, though the ones that do exist intersect the properties. The Oregon properties are not near any large scale mapped faults.

Methods

Data

The creation of the manual landslide inventory took place on location at the partner organization's offices. Data used for the manual and automated landslide inventory map creation were derived from LiDAR DEMs (Digital Elevation Models). Multiple LiDAR sets were used for complete coverage of the study area; much of the property is covered by proprietary LiDAR imagery and where unavailable, publically available LiDAR from the Puget Sound LiDAR Consortium (PSLC) was used. PSLC data is available in 6 foot resolution. Proprietary imagery in the Shelton area is 3 feet, proprietary Morton area imagery is 3.28 feet (originally collected at 1 meter), proprietary Brooklyn area imagery is 3 feet, and all Oregon LiDAR is 3 feet resolution. All Washington LiDAR files were reprojected into the NAD_1983 Washington State Plane South feet projection. All Oregon files were reprojected into the NAD_1983 Oregon State Plane North feet projection.

Manual landslide inventory

The process for creating the manual landslide inventory involved visual identification of landslide morphology and digitization of slide boundaries and scarps. All processing was performed in ESRI ArcMap. The procedure for mapping of the landslides was modified from the Oregon Department of Geology and Mineral Industries (DOGAMI) protocol for landslide identification and mapping (Burns & Madin, 2009). The DOGAMI methods are designed to maximize the visibility of landslide morphology such as changes in elevation and slope. This is accomplished through layering of a base colorized topographic hillshade, a slope map indicating slopes greater than 45°, and contours at intervals of 2, 5, and 10 feet dependent on the scale of the area being examined. Figure 1 presents this imagery in varying states of the overlays used. A satellite imagery basemap was also used to review for patterns when the LiDAR was insufficient.

These layers contributed to easier identification of deep-seated landslide terrain features according to failure styles as defined by Varnes (1978). These features include head and flank scarps, hummocks, rotated benches, sag ponds, and zones of depletion and accumulation. For each slide identified, a boundary was digitized as well as a head scarp (if visible) and any internal scarps observed. Other characteristics observed about each slide are recorded in Table 1.

Table 1.

Summary of the attribute table created during the manual landslide identification process.

Attribute	Attribute Description
Slide_ID	Designated by the county location and the order of identification
Type_Move	Style of failure motion: Translation, Rotation, Complex
Age	Relative age of the slide, Uncertain, Ancient, or Modern; determined by distinct changes in roughness over small areas and any overlapping features
Geol	The dominant underlying geology
Confidence	Degree of confidence of past slide motion: High, Moderate, Low
Comment	Observations of specific morphology and any features not already included

As referenced in Table 1 and throughout the manual classificaiton, styles of failure were determined by resemblance to descriptions from Varnes (1978). These include rotational, translational, and complex slides. Rotational slides are characterized by a concave upward slide surface and cohesive tilted benches. Translational slides are characterized by a planar slide surface. Complex slides can be any combination of these two styles of failure. The relative age and degree of weathering are approximated based on the distinctness of features such as scarps relative to the ground surface adjacent to them.

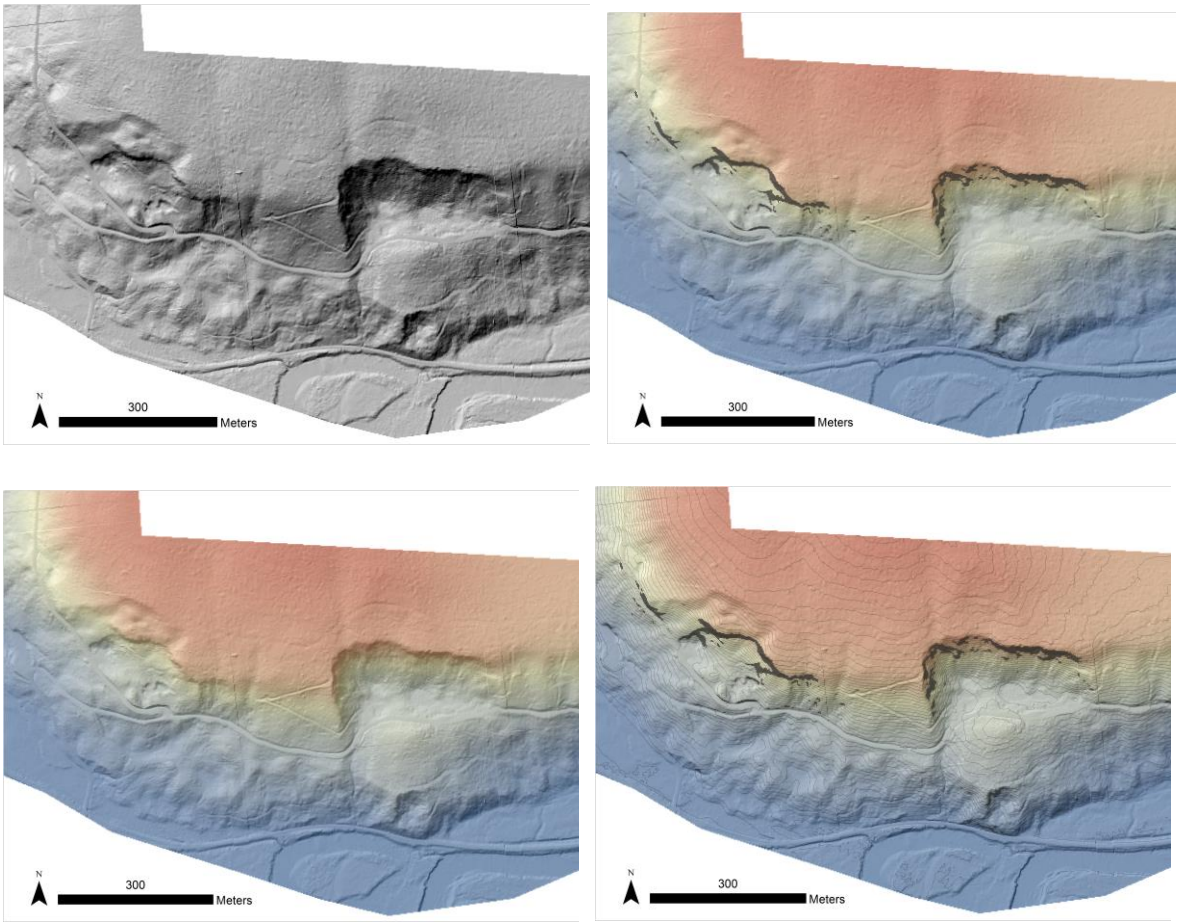

Figure 1. Products used for manual identification of landslides. Clockwise from upper left: bare earth hillshade, hillshade with elevation-derived color gradient (blue for low and red for high), color elevation gradient and slopes >45° shaded a dark gray, all aforementioned products and 10 foot contours (interval used varied and dependent on the scale of the area being evaluated).

Automated landslide inventory

I used a continuous wavelet transform (CWT) as set forth by Booth et al. (2009) for the automated identification of deep seated landslides in western Washington and Oregon. I selected this method to apply to the study area due to the similarity to the prior study in both setting and data available.

The CWT is a signal processing method used to simplify and summarize complex signals. Booth et al. (2009) use a "Mexican hat" wavelet CWT as it approximates the form of a landslide hummock. Each iteration of processing identified a range of wavelengths produced by landslides within the parcel. The wavelet transform is applied to this range of frequencies to calculate a spectral power sum. Training areas of failed and unfailed terrain are selected to identify and create a cutoff value of the spectral power sum. Pixels with a spectral power sum higher than the cutoff are designated landslide and those below are designated non-landslide. Similar to the manual landslide raster files, the output of this code is a binary raster identifying terrain as either landslide or non-landslide.

Preparation of the data was performed in ArcMap and processing for landslide identification was performed in MATLAB using the script from Booth et al. (2009) (Appendix 1). In ArcMap, LiDAR DEMs were clipped around properties to create parcels of manageable file size and processing time, to maintain geographic similarity, and to include a buffer of land outside the properties where possible. Where property boundaries required multiple files (due to large areas), the files were clipped with overlapping areas. Training patches of failed and unfailed terrain were selected on the DEM files to identify a characteristic wavelength for each property. Properties on which no landslides had been identified were excluded from the automatic classification as the training patch selection is required for further identification. Where possible, areas that have been excessively altered, such as roads and artificially graded areas were avoided when selecting training areas for unfailed terrain. Discrete locations were selected from each property as training patches, in an effort to accommodate for changes in landslide causes such as geology, vegetation, or groundwater. Where processing files overlapped, training areas were selected from the overlap area to maintain uniform processing between properties. An edge buffer equal to 4*wavelength cutoff is applied to all processed parcels to eliminate edge effects.

Results

The manual review of the study area identified 470 individual landslides and 1,829 total scarps. These deposits range in size from .31 acres to 1013.9 acres and cover a total area of 7,936.27 acres. The breakdown by region is presented in Table 2.

Table 2.
Statistics for the manual landslide inventory

	Shelton	**Brooklyn**	**Morton**	**Oregon**
Total area (acres) evaluated	39,475.73	75,948.56	112,556.63	103,478.55
Average plot area (acres)	1,462.06	1,615.93	2,206.99	2,586.96
Area (acres) identified as landslide	326.87	1,221.32	3,656.08	2,732.01
Percent landslide	0.83	1.61	3.25	2.64
Total number of slides	64	154	116	136
Landslide Density (Slides/Acre)	.0016	.002	.001	.001
Smallest slide (acres)	0.356	0.317	0.766	1.46
Largest slide (acres)	570.8	430.73	1013.9	775.34
Average slide size (acres)	22.7	54.76	67.83	68.2
Most abundant slide size (acres)	0-39.5	0-44.5	0-101.3	0-79.1

The manual method of inventory creation relied on the expression of morphologic features such as scarps and hummocks. These constraints lent itself to mapping deposits with a clear point of origin that were oblong and generally lobate. Examples of some of the identified slides are presented in Figures 2 and 3. The slides occurred both in isolation and in clusters. Where possible, the boundaries of adjacent slides were included in the digitization process. Where these flank scarps could not be identified, or where it appeared they might belong to the same complex, a single body was digitized (Figure 2).

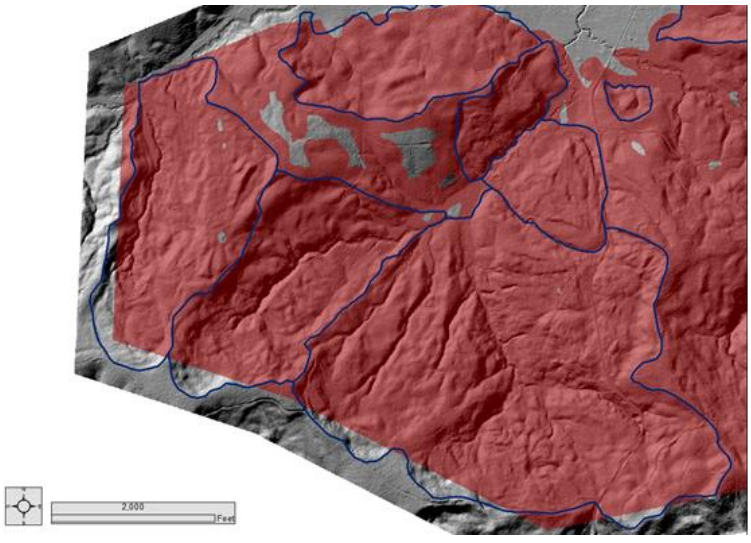

Figure 2. Example of landslide areas identified in the manual review and automated processing. Borders along flank scarps have been drawn here to distinguish between distinct landslide complexes.

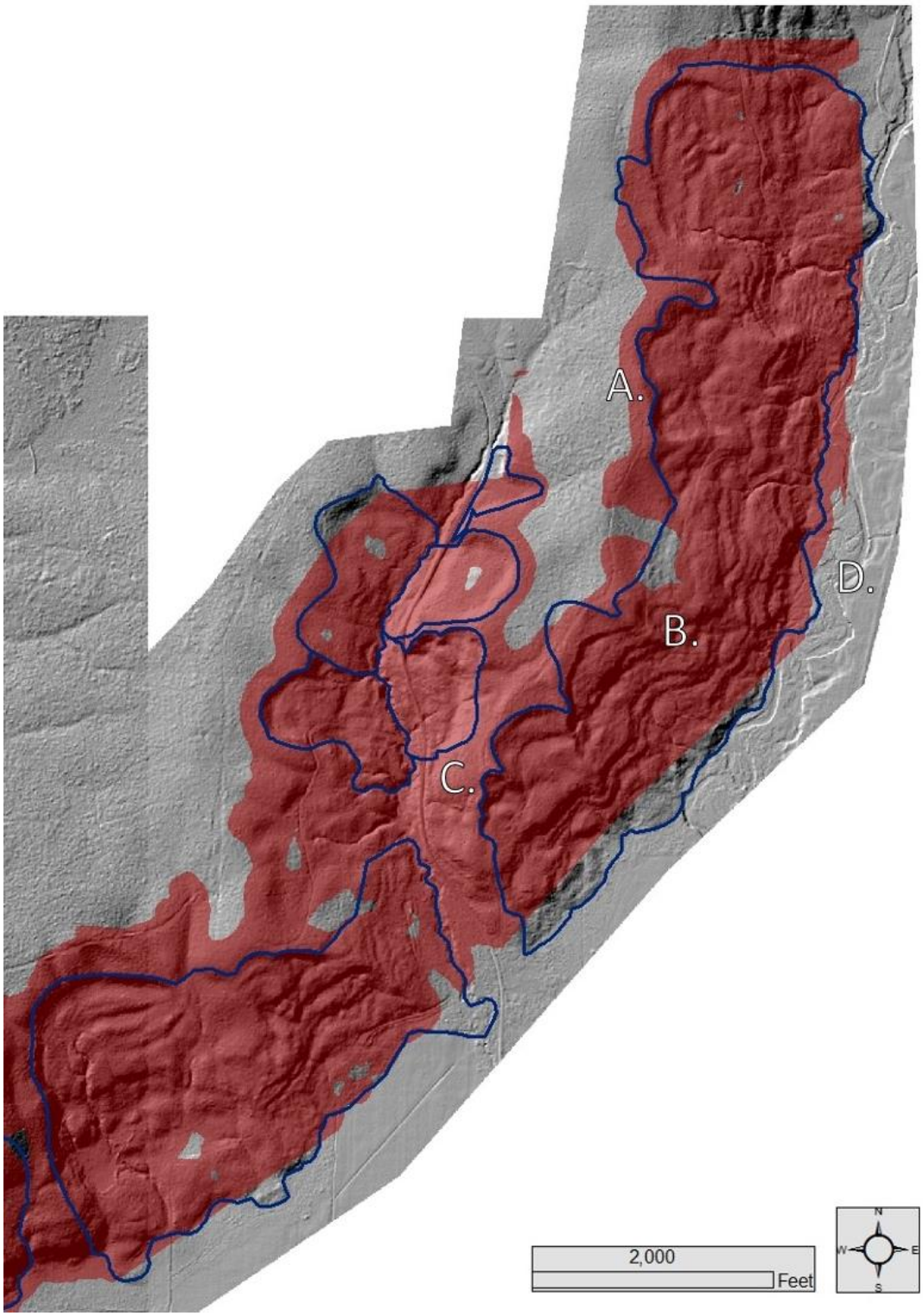

Figure 3. Example image of the manual and automated inventory results, overlain on a hillshade raster. Dark blue outlines slides identified in the manual review. Red indicates areas that were designated landslide terrain by automated processing. Examples of head scarps (A.), internal scarps (B.), roads (C.), and river channels (D.) are indicated.

Because the CWT analysis does not delineate the boundaries of individual landslides, areas are reported as "landslide terrain" rather than as individual slide statistics. Examples of the automated review results are also included in Figures 2 and 3. The automated methods identified distinct 9,366 areas of landslide terrain. These areas range in size from .000764 ac to 9,503.15 ac and cover a total area of 22,492.39 ac. The regional summary of the automated inventory is presented in Table 3.

Table 3.
Statistics for the automated (CWT) landslide inventory

	Shelton	**Brooklyn**	**Morton**	**Oregon**
Total area (ac) evaluated	39,475.73	75,948.56	112,556.63	103,478.55
Average plot area (ac)	1,462.06	1,615.93	2,206.99	2,586.96
Area (ac) identified as landslide	1,234.97	14,398.30	12,224.62	10,234.98
Percent landslide	3.13	18.96	10.86	9.89
Number of slide areas	957	1009	3513	3887
Smallest slide area (ac)	0.000825	0.00122	0.000764	0.000909
Largest slide area (ac)	1762.23	7106.23	9503.15	4120.78
Average slide area size (ac)	8.92	35.26	8.6	6.5

The total area of landslides identified in the Shelton area using CWT is 3.77 times greater than the area identified manually. The Brooklyn CWT area is 11.79 times greater, Morton CWT area is 3.34 times greater, and in Oregon the CWT identified an area 3.75 times greater.

To compare the results of the automated landslide inventory with the manual inventory maps, I calculated the mismatch between inventory maps. This index, calculates a spatial disagreement between the methods. The equation used for this calculation was taken from Carrara et al. (1992):

$$E = \frac{(A_1 \cup A_2) - (A_1 \cap A_2)}{(A_1 \cup A_2)}, 0 \leq E \leq 1 \quad (1)$$

where A_1 and A_2 indicate the total landslide area in the two inventories. "Matching" is the inverse of this index and indicates the total area that both methods identified as landslide terrain.

The final "disagreement" using Eq. 1 between the methods for each of the cumulative areas was calculated comparing the union, the cumulative area identified as landslide terrain, and the intersection, the area identified by both methods as landslide terrain. For the Shelton area this yields an error of 89% and 11% matching; for Brooklyn error is 83% and matching is 17%; for Morton error is 80% and matching is 20%; and for Oregon error is 73% and matching is 27%.

Discussion

The inventory maps created using these two methods resulted in two fundamentally different interpretations identifying locations of potential deep seated landslides. This difference may be attributed to the fact that the manual method is better suited to identify single occurrences, whereas the CWT is better suited to identify large areas that may have been affected. The most significant challenge presented during the completion of the manual inventory was distinguishing between old heavily weathered landslide complexes and drainage basins. Often these would overlap, and in these cases discretion was used to digitize only landslides that showed clear morphologic features and not simply indicative terrain.

There is a large degree of overlap between the two inventory maps. Average mismatch values are high due to the much larger area that the automated method classified as landslide that the manual review did not. This includes areas such as fluvial channels, modified surfaces such as roads, and other linear features. The automated review tended to characterize these features as landslides because of their potential resemblance to a scarp, and the rapid change in topography. Distinct examples of this misclassification can be seen in Figure 4. This observation aligns with observations made by Booth, et al. (2009). The automated review can be refined and mismatch potentially reduced by adjusting parcel size, masking roads and rivers, and testing for the highest accuracy training areas.

Many of the final imagery parcels resulted in a low spatial disagreement. Figure 5 presents some of these images. In these areas, both the manual an automated inventories designated much of the same groundcover as failed terrain. Though the landslide terrain identified by the automated inventory tends to extend beyond the bounds of the manual review, there is more agreement within the manually identified slides.

Other imagery from the results of both inventories characterized the extent of landslides similarly, however, the automated methods failed to identify swaths within the manually identified bounds, leaving 'holes' in the automated overlay (Figure 6). These holes may be a result of undisturbed ground surface on rotated benches, poorly selected training areas, or poorly processed LiDAR imagery.

Imagery from smaller parcels or parcels on which only smaller slides were identified during the manual review tended to be indiscriminately classified as landslide terrain by the automated process (Figure 7). This produces a high degree of disagreement between the methods, noting that the areas designated slide terrain by the automated review tend to occupy the extent of the parcel being evaluated.

The automated review produced several broad patterns that can be considered only partially accurate in identification of landslides (Figure 8). These patterns generally failed to align with the manual review and were expressed as scattered, isolated, small features and as a tendency to misidentify channels and other linear features.

The final, and perhaps most distinct, pattern observed across the results of the automated review is the juxtaposition of adjacent tiles that were processed separately (Figure 9**)**. This distinction was made for two reasons: spatial area (and thus corresponding file size) and the presence of a

manually identified slide (which is necessary to run the automatic evaluation) which sometimes required large areas to be split along a boundary to include the slide.

Summary and Conclusion

The demands of the logging industry and the susceptibility to landslides in the Pacific Northwest create a clear need for landslide inventories. Through the identification of past landslides on the partner organization's properties, I constructed two landslide inventories from LiDAR imagery, manual and automated. The manual review is built on the recognition and interpretation of characteristic landslide morphology. The automated CWT relies on the presence of a dominant spatial frequency and the identification of the range of characteristic frequencies. The results of these inventories were compared for their spatial alignment and differences in spatial morphology.

The process for manual landslide inventory creation is inherently subjective and can be cumbersome. However, review of the results throughout the inventory creation process increases the veracity of the manual results. Automated CWT inventories require further review of results for accuracy. This inventory is dependent of factors inherent in the landscape and their representations in the LiDAR imagery. These factors range from controls on failure styles, relative age of failure, and degree of weathering. Furthermore, this method assumes that these factors are uniform across each parcel and share a characteristic wavelengths, making the results of the CWT dependent of the selection of the areas for training patches. Quality and resolution of LiDAR remains the most important aspect of creating a landslide inventory.

Manual office techniques remain the most reliable means of landslide identification. Where any landslide inventory exists or in a small study area, newly identified or occurring slides can be easily added to the existing map. For larger areas with no existing inventory, an automated method may be considered. Several adjustments to the CWT analysis can improve on the results of an automated inventory. Assuring quality LiDAR imagery is fundamental to this process. Masking of commonly misidentified features such as roads and river channels will remove these areas from the processing and narrow the available frequency band. With each parcel that is processed, training patches and parcel size should be adjusted to achieve the greatest degree of matching. Geologic diversity should be minimized by parcel as it is a control on failure style and characteristic wavelength generation.

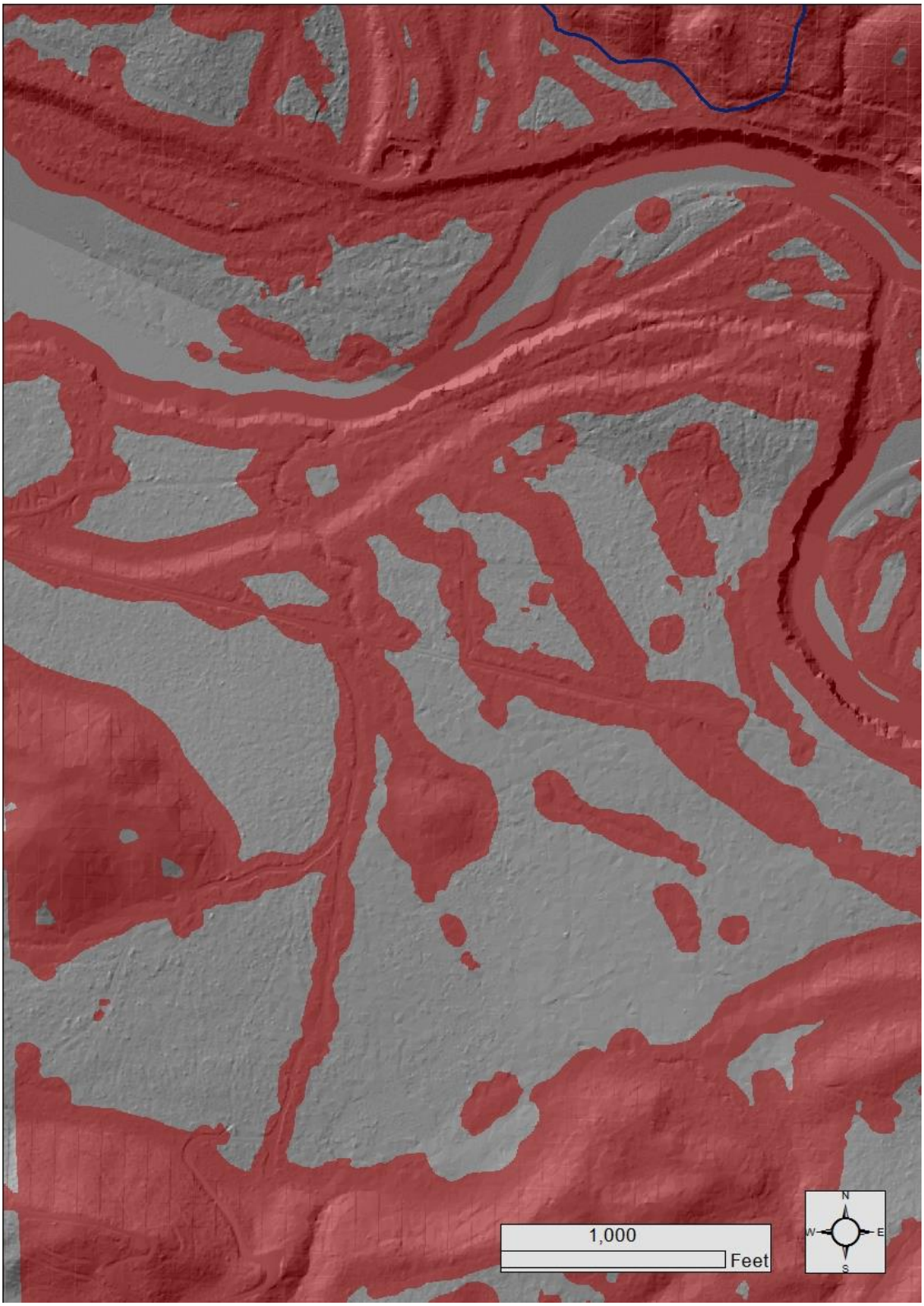

Figure 4. Imagery with results of automated classification indicated by red overlay. Here, roads and some fluvial channels are misclassified as landslide terrain. These are identified as the thin elongate portions of the overlay in which linear 'divots' are observed.

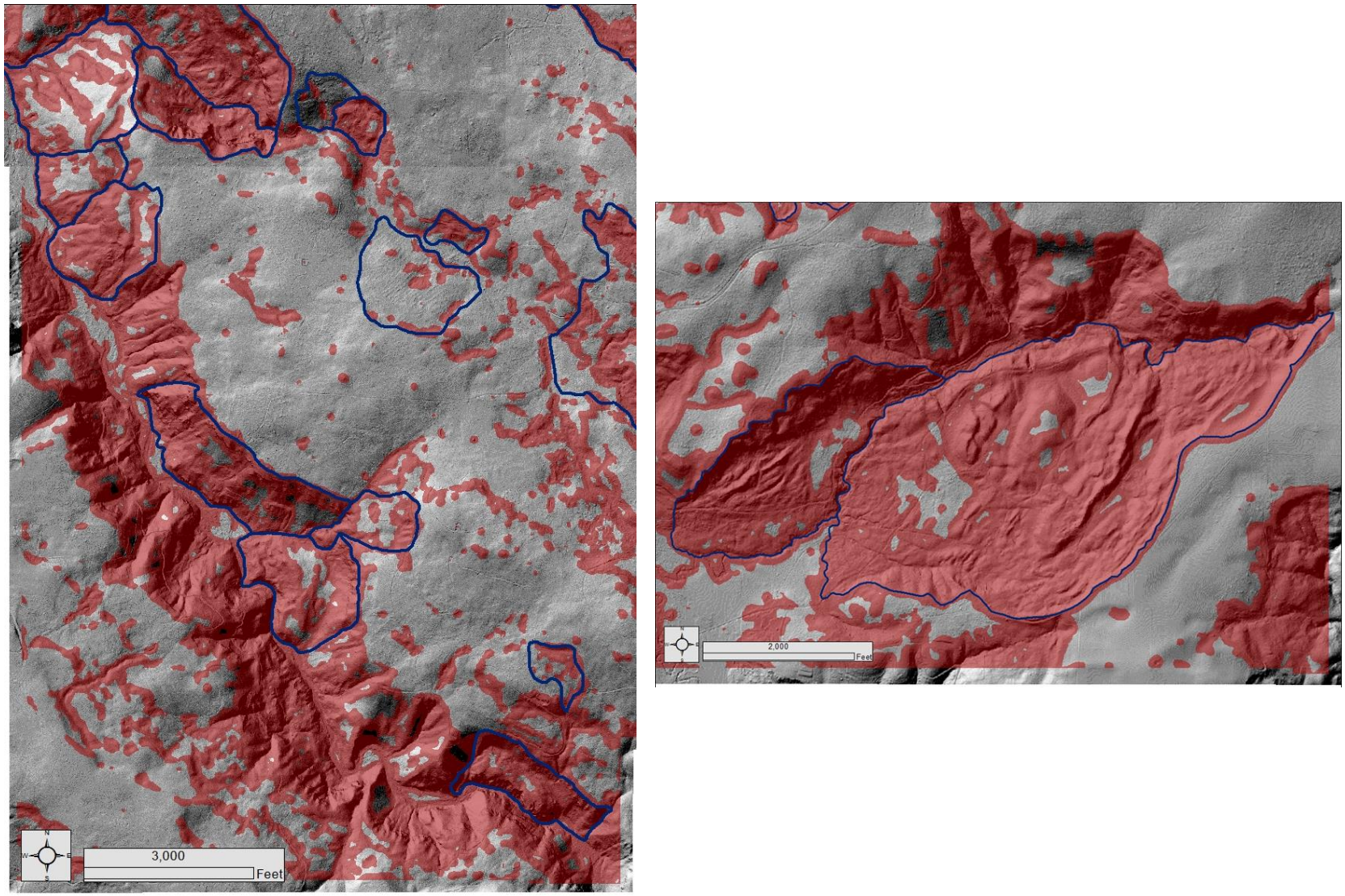

Figure 5. Imagery displaying landslide terrain as designated by the manual (dark blue) and automated review (red overlay). These are examples of locations where the manual and automated reviews were largely in agreement in areas designated as landslide terrain.

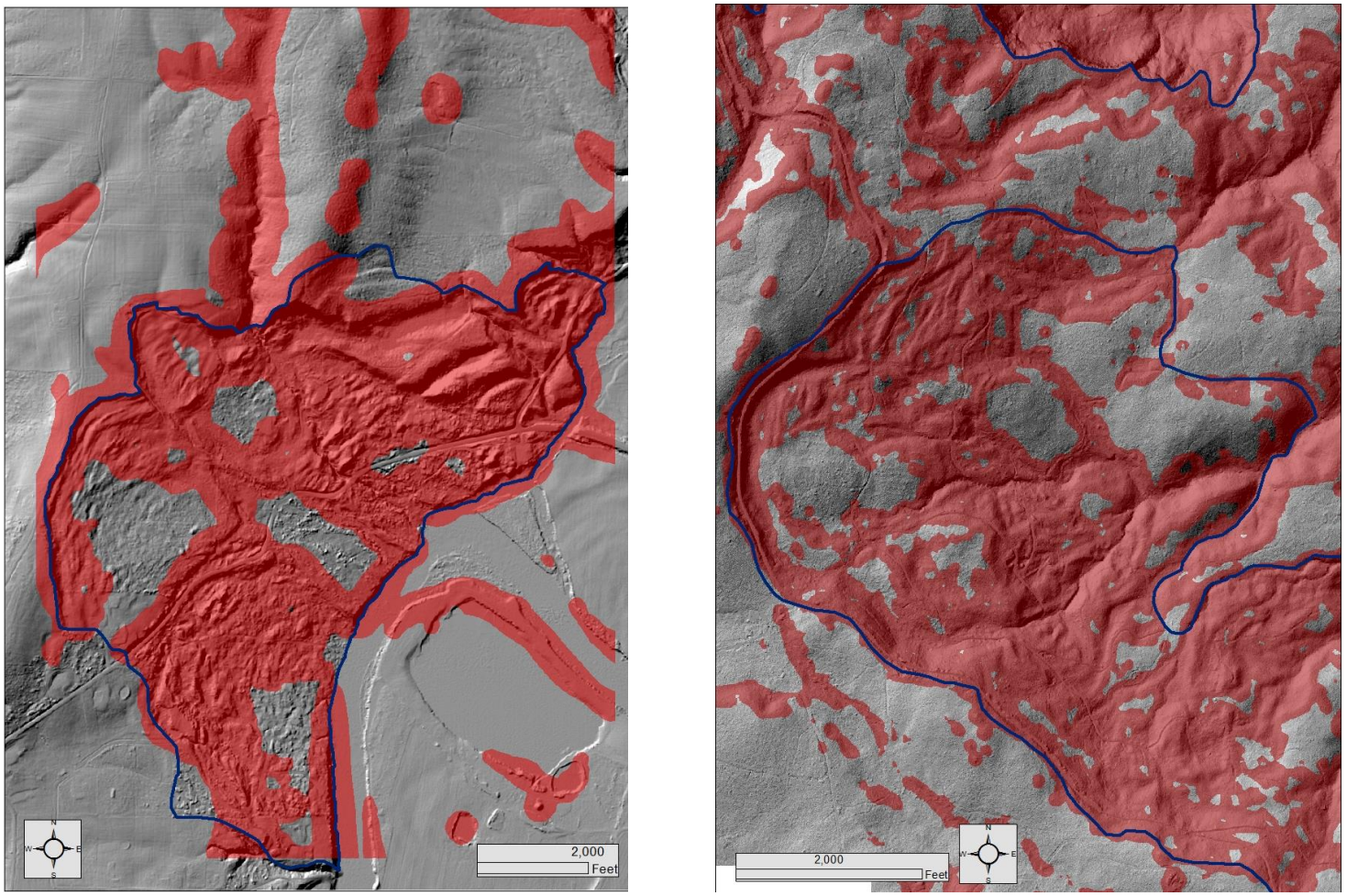

Figure 6. Example imagery featuring automatically designated terrain (red overlay) with interior 'holes'. The extent of the slide terrain is assigned similarly by both methods, but the automated methods fail to identifiy the whole of the manually identified (dark blue) slide terrain.

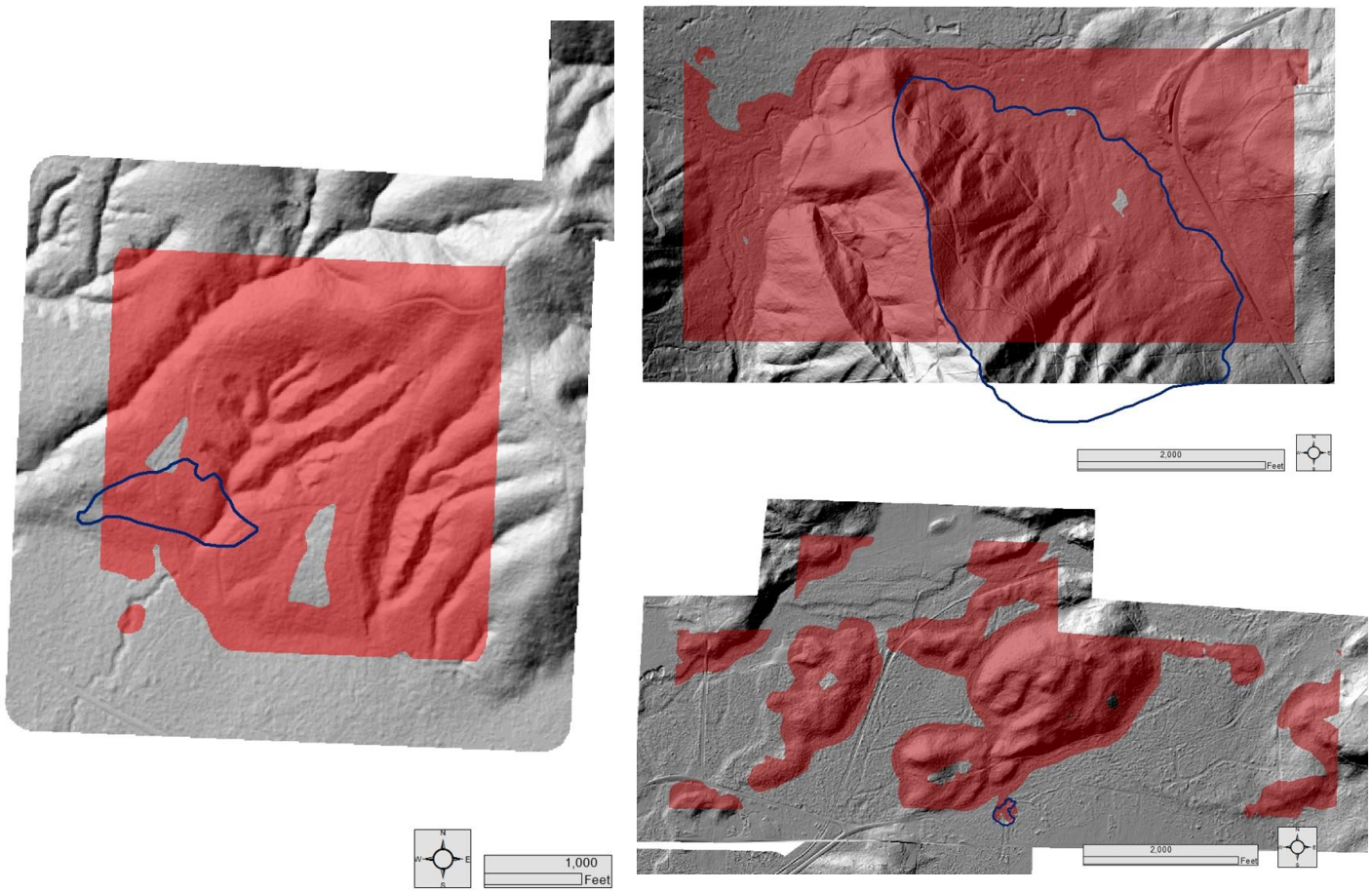

Figure 7. Examples of small parcels or parcels with minimal area identified as slide terrain by the manual review. These situations produced a high degree of disagreement between the methods.

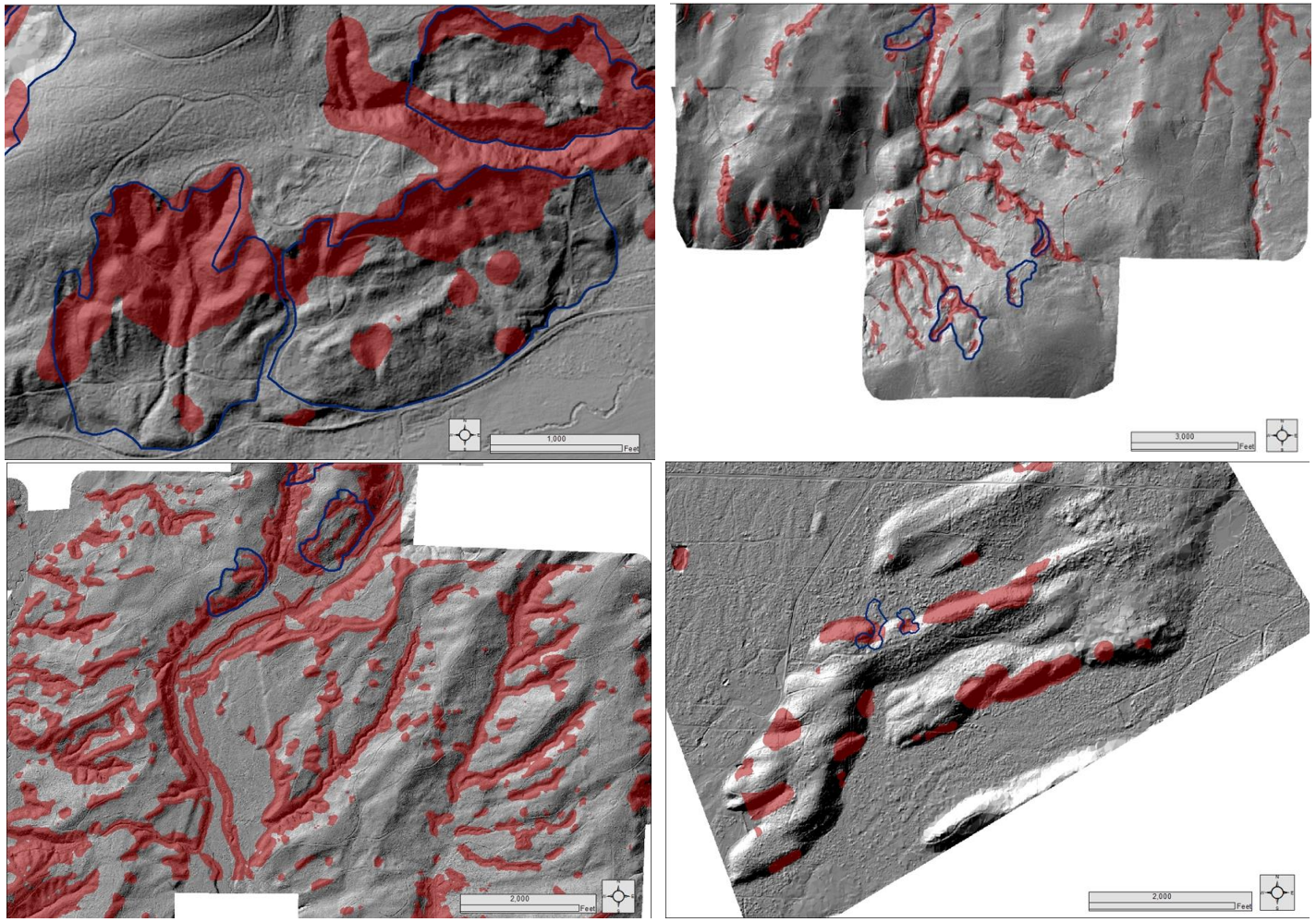

Figure 8. Examples of poorly classified landslide terrain from the automated review (red overlay). In these cases, the training areas from the manual review (dark blue) tended to be small, limiting the terrain to which the automatic classification would identify.

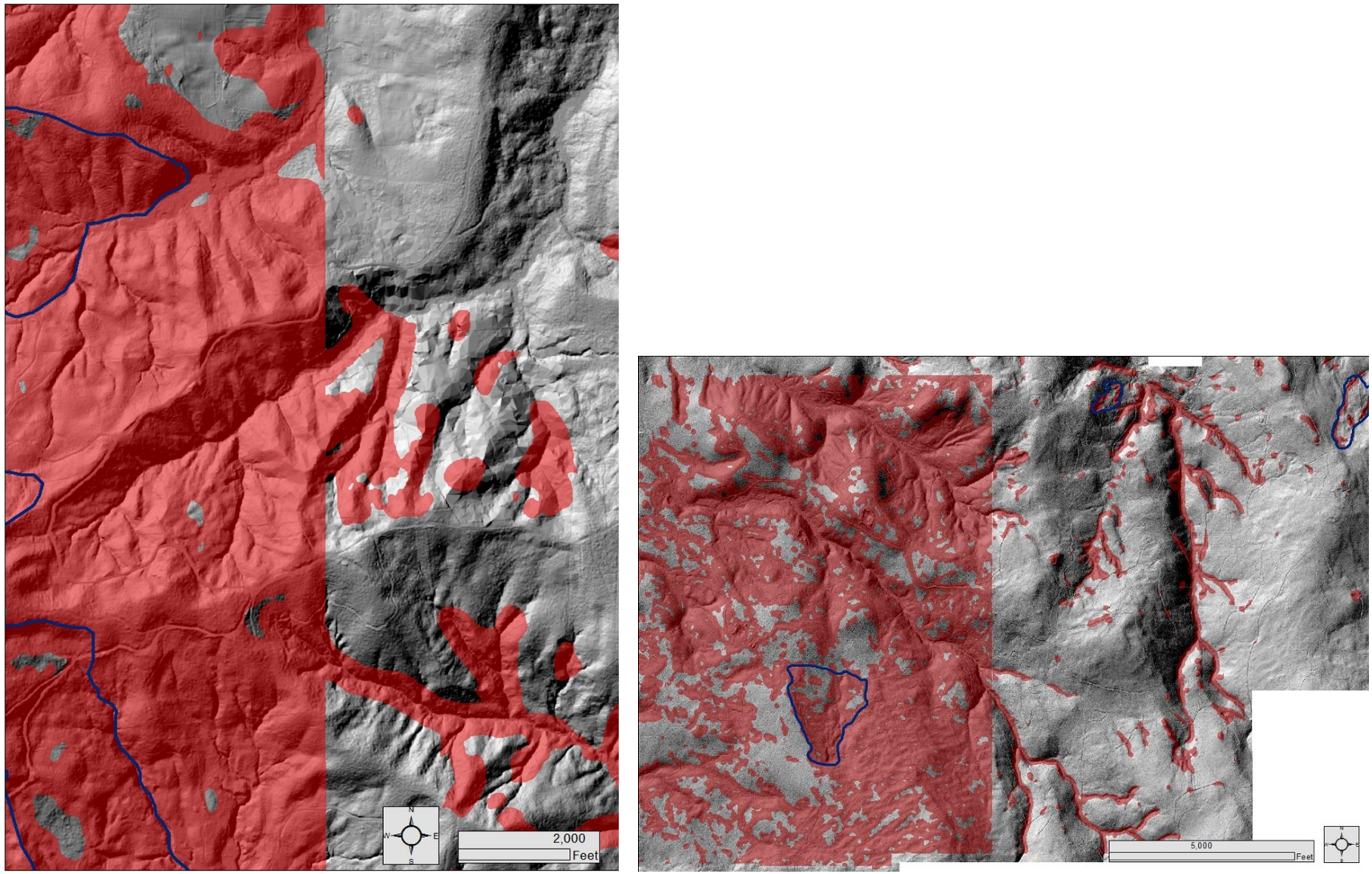

Figure 9. Examples of parcels that were split for automated processing. Due to the selection of different training areas (manually identified in dark blue) or the same training area applied to a different parcel, these scenarios produced the most contrasting automated results (red overlay).

Works Cited

Berti, M., Corsini, A. and Daehne, A., 2013, Comparative analysis of surface roughness algorithms for the identification of active landslides. Geomorphology, v. 182, pp.1-18. https://doi.org/10.1016/j.geomorph.2012.10.022.

Booth, A.M., Roering, J.J., and Perron, J.T., 2009, Automated landslide mapping using spectral analysis and high-resolution topographic data: Puget Sound lowlands, Washington, and Portland Hills, Oregon: Geomorphology, v. 109, p. 132-147, doi:10.1016/j.geomorph.2009.02.027.

Borguis, A.M., Chang, K., and Lee, H.Y., 2007, Comparison between automated and manual mapping of typhoon-triggered landslides from SPOT-5 imagery: International Journal of Remote Sensing, v. 28, p. 1843-1856, doi: 10.1080/01431160600935638.

Brardinoni, F., Slaymaker, O. and Hassan, M.A., 2003, Landslide inventory in a rugged forested watershed: a comparison between air-photo and field survey data. Geomorphology, 54(3), pp.179-196. https://doi.org/10.1016/S0169-555X(02)00355-0.

Burns, W.J., and Madin, I.P., 2009, Protocol for Inventory Mapping of Landslide Deposits from Light Detection and Ranging (LiDAR) Imagery: Oregon Department of Geology and Mineral Industries Special Paper 42, 36 p. http://www.oregongeology.org/pubs/dds/slido/sp-42_onscreen.pdf

Carrara, A., M.Cardinali, F. Guzzetti., 1992, Uncertainty in assessing landslide hazard and risk, ITC Journal, 2, pp 172-183.

Cruden,D.M., Varnes, D.J., 1996, Landslide Types and Processes, Special Report , Transportation Research Board, National Academy of Sciences, 247:36-75.

Van Den Eeckhaut, M., Poesen, J., Verstraeten, G., Vanacker, V., Moeyersons, J., Nyssen, J. and Van Beek, L.P.H., 2005, The effectiveness of hillshade maps and expert knowledge in mapping old deep-seated landslides, Geomorphology, 67(3), pp.351-363, https://doi.org/10.1016/j.geomorph.2004.11.001

Farina, P., Colombo, D., Fumagalli, A., Marks, F., Moretti, S., 2006, Permanent scatters for landslide investigations: outcomes from the ESA-SLAM project. Engineering Geology 88, 200–217. https://doi.org/10.1016/j.enggeo.2006.09.007.

Galli, M., Ardizzone, F., Cardinali, M., Guzzetti, F., and Reichenbach, P., 2008, Comparing landslide inventory maps: Geomorphology, v. 94, p. 268-289, doi:10.1016/j.geomorph.2006.09.023.

Furbish, D.J., and Rice, R.M., 1983, Predicting landslides related to clearcut logging, Northwestern California, USA: Mountain Research and Development, v. 3, p. 253-259, doi: 10.2307/3673019.

Logan, R. L., 1987, Geologic Map of the Chehalis River and Westport Quadrangles: Washington Division of Geology and Earth Resources, Open File Report 87-8.

Logan, R.L., 2003, Geologic Map of the Shelton 1:100,000 Quadrangle. Washington, State of Washington, Department of Natural Resources, Division of Geology and Earth Resources, Open File Report, 15.

Malamud, B.D., Turcotte, D.L., Guzzetti, F. and Reichenbach, P., 2004, Landslide inventories and their statistical properties: Earth Surface Processes and Landforms, v. 29, p. 687–711, doi: 10.1002/esp.1064.

Mondini, A.C., Guzzetti, F., Reichenbach, P., Rossi, M., Cardinali, M., Ardizzone, F., 2011, Semi-automatic recognition and mapping of rainfall induced shallow landslides using satellite optical images, Remote Sensing of Environment 115, 1743–1757, doi:10.1016/j.rse.2011.03.006.

Montgomery, D.R., Schmidt, K.M., Greenberg, H.M., and Dietrich, W.E., 2000, Forest clearing and regional landsliding: Geology. v. 28, p. 311-314, doi:10.1130/0091-7613(2000) 28<311:FCARL>2.0.CO;2.

Phillips, W. M., 1987, Geologic Map of the Mount St Helens Quadrangle, Washington and Oregon: Washington Division of Geology and Earth Resources, Open File Report 87-4.

Schasse, H. W., 1987, Geologic Map of the Centralia Quadrangle, Washington: Washington Division of Geology and Earth Resources, Open File Report 87-11.

Stumpf, A., Kerle, N., 2011, Object-oriented mapping of landslides using Random Forest, Remote Sensing of Environment 115 (10), 2564–2577, doi:10.1016/ j.rse.2011.05.013.

Van Den Eeckhaut, Poesen, M.J., Verstraeten, G., Vanacker, V., Moeyersons, J., Nyssen, J., and van Beek, L.P.H., 2005, The effectiveness of hillshade maps and expert knowledge in mapping old deep-seated landslides: Geomorphology, v. 67, p. 351-363, doi:10.1016/j.geomorph.2004.11.001.

Varnes, D. J. 1978. Slope movement types and processes. In Special Report 176: Landslides: Analysis and control (Eds: Schuster, R.L and Krizek, R.J), Transportation and Road research board, National Academy of Science, Washington D.C. 11-33.

Walsh, T. J., 1987, Geologic Map of the Astoria and Ilwaco Quadrangles, Washington and Oregon: Washington Division of Geology and Earth Resources, Open File Report 87-2.

Appendix 1.

See MESSAGe digital library for MATLAB script from Booth et al., 2009.